

# Nanoscale

Accepted Manuscript



This is an *Accepted Manuscript*, which has been through the Royal Society of Chemistry peer review process and has been accepted for publication.

*Accepted Manuscripts* are published online shortly after acceptance, before technical editing, formatting and proof reading. Using this free service, authors can make their results available to the community, in citable form, before we publish the edited article. We will replace this *Accepted Manuscript* with the edited and formatted *Advance Article* as soon as it is available.

You can find more information about *Accepted Manuscripts* in the [Information for Authors](#).

Please note that technical editing may introduce minor changes to the text and/or graphics, which may alter content. The journal's standard [Terms & Conditions](#) and the [Ethical guidelines](#) still apply. In no event shall the Royal Society of Chemistry be held responsible for any errors or omissions in this *Accepted Manuscript* or any consequences arising from the use of any information it contains.

Cite this: DOI: 10.1039/c0xx00000x

www.rsc.org/xxxxxx

ARTICLE TYPE

## Carbon Nanodots as Ligand Exchange Probes in Au@C-dot Nanobeacons for Fluorescent Turn-on detection of biothiols

Sonam Mandani, Bhagwati Sharma, Deepa Dey and Tridib K. Sarma\*

*Received (in XXX, XXX) Xth XXXXXXXXX 20XX, Accepted Xth XXXXXXXXX 20XX*

DOI: 10.1039/b000000x

Au nanoparticle-carbon dot core-shell (Au@C-dot) nanocomposites were synthesized in aqueous medium at room temperature using the carbon dots as reducing agents themselves. The carbon nanodots also function as an effective stabilizer by forming a thin layer surrounding Au nanoparticles (Au NPs) similar to self-assembled monolayers. Ligand exchange with thiol containing biomolecules resulted in the release of carbon dots from the Au NP surface leading to enhancement of fluorescence. Simultaneously the agglomeration of Au NPs stimulated by the interaction of biothiols led to changes in the surface plasmon properties of Au NPs. A detailed spectroscopic investigation revealed a combination of static and dynamic quenching being involved in the process. Thus, the Au nanoparticle-carbon dot composite could be used as a dual colorimetric and fluorometric sensor for biothiols ranging from amino acids, peptides, proteins, enzymes etc. with a detection limit of 50 nM.

### Introduction

Metal-ligand interactions have traditionally been utilized as the driving force in assembling nanoparticle based sensors affording high selectivity and operability in aqueous medium.<sup>1-5</sup> Plasmonic nanostructures such as those of Au have gained tremendous importance as colorimetric reporters because of their excellent and distinctive properties such as high extinction coefficients in the visible region and distance dependent optical properties.<sup>6-9</sup> The distinct color of the colloidal Au in dispersed (red) and aggregated form (blue) has led to development of efficient nanosensors for various heavy metals, anions and biomolecules.<sup>8-17</sup> Generally, these "smart" nanosensors are based on assembling nanoparticles with tailored functional groups that selectively bind the analyte, leading to 1D, 2D or 3D interparticle bridging assemblies. This results in optical changes induced by short and long range interactions of surface plasmon resonance (SPR) of individual nanoparticles. On the other hand ligand displacement reactions, i.e. exchange of surface stabilizing agents by analytes with higher affinity for the nanoparticle surface could potentially be used for biological recognition events, if the specific marker of interest leads to interparticle crosslinking.<sup>18-21</sup> Additionally, if the ligand exchange process could lead to enhancement of fluorescence inherent to the displaced surface stabilizing agents, then the nanosensor could function as a dual probe detector, both colorimetric and fluorometric, for the sensitive analysis of specific biomolecules.

Carbon dots (C-dots) are an emerging class of carbon nanomaterials owing to their splendid fluorescence property, good biocompatibility, water solubility, photostability and energy conversion abilities.<sup>22-30</sup> The tremendous attention to this tiny water soluble form of carbon could be attributed to their role as

non-toxic and eco-friendly alternative to semiconductor quantum dots in various applications ranging from electronics, catalysis, bioimaging and drug delivery.<sup>22-34</sup> Their easy method of synthesis, surface passivation and tunable photoluminescence properties has led to the development of a number of fluorometric sensors.<sup>35-39</sup> The upconversion luminescence properties of these nanolights have been utilized for the fabrication of photocatalytic system to harness the full spectrum of sunlight.<sup>23-25</sup> The beauty of carbon dot is that depending on the source and the procedure used for its synthesis, the functional groups on its surface can be tailored. With the abundant presence of carboxylic moiety on the surface, C-dots could function as a reducing as well as stabilizing agents in the synthesis of metallic nanoparticles such as Au and Pd,<sup>27,40-42</sup> similar to other carboxyl rich ligands such as citrates, ascorbates etc. In this process, C-dots form a shell around the metal nanoparticle that might function similar to a self-assembled monolayer of a stabilizing agent.

Here, we report the development of Au nanoparticle-carbon dot core-shell composites (Au@C-dot) as both colorimetric and fluorometric nanosensor for biothiols which works through a combination of ligand exchange and Förster resonance energy transfer (FRET) phenomena. The mechanism is based on the ligand exchange reactions on Au nanoparticles (Au NPs), where C-dots are replaced by the biothiols through the formation of stronger Au-S bond. This leads to enhancement of fluorescence emission inherent to C-dots. Additionally, interaction of thiol molecules with Au NPs leads to their agglomeration, thus altering their optical properties.<sup>43-45</sup> Both these phenomena have been exploited for the development of Au@C-dot nanocomposites as colorimetric as well as fluorometric sensor. Numerous thiol containing biomolecules such as cysteine, glutathione etc. are crucial for the regulation of a number of biological processes in

the human body. Hence, monitoring of these thiol compounds is of great importance for diagnosis of diseases.<sup>46,47</sup>

## Experimental Section

### Reagents

Hydrogen tetrachloroaurate (HAuCl<sub>4</sub>), D-penicillamine and Bovine serum albumin (BSA) were purchased from Sigma-Aldrich.  $\beta$ -carotene, glutathione, L-amino acids (cysteine, methionine, lysine, arginine, glutamic acid, aspartic acid, alanine and leucine) and the enzymes (urease, pepsin and glucose oxidase) were supplied by Sisco Research Laboratories, India. Glucose and fructose were bought from Merck, India. Becozyme C forte and Xtraglo tablets were obtained from Piramal Healthcare and Sun Pharma, India respectively. The chemicals were used as received and their solutions were prepared in Milli Q water.

### Synthesis of Carbon dots

In a typical procedure,  $\beta$ -carotene at a concentration of 0.5mg/mL was dispersed in water in a sealed glass tube which was subjected to microwave irradiation at power 150 watts and temperature 150 °C for 45 minutes. This resulted in a pale yellow dispersion of luminescent C-dots. The solution was filtered through a Whatman filter paper to remove any insoluble part before using for further experiments.

### Preparation of Au@C-dot composite

The Au@C-dot composite was obtained by addition of 40  $\mu$ L of a 30 mM HAuCl<sub>4</sub> solution to a C-dot solution (2.0 mL) at room temperature. The resulting mixture was allowed to stand for 30 minutes when it turned pink indicating the formation of Au NPs.

### Assay of biothiols

2 mL of Au@C-dot solution was titrated with aliquot of 5  $\mu$ L of 1 mM solution of different thiols. The solutions were equilibrated for 5 mins at room temperature before recording the spectra.

### Assay of biomacromolecules

The proteins/enzymes were dissolved in PBS buffer of pH 7.4 at a concentration of 2.0 mg/mL and small aliquots were incubated with Au@C-dot solution for 15 mins before recording the spectrum. For the assay for pharmaceutical samples, the tablets were crushed and dissolved in water (1.0 mg/mL). The solution was filtered and aliquots were incubated with Au@C-dot.

### Instrumentation

Microwave irradiation experiments were performed in a focused microwave CEM discover reactor. A Varian Cary 100 Bio spectrophotometer was used for UV-visible measurements. Emission spectra were recorded using a fluoromax-4p fluorometer from Horiba (Model: FM-100). Powder X-ray diffraction patterns (XRD) were obtained on a Bruker D8 Advance diffractometer with Cu K $\alpha$  source (wavelength of X-rays was 0.154 nm). A JEOL JEM-2100 microscope was used to obtain the transmission electron microscopy (TEM) images at an operating voltage of 200 kV. FTIR spectra were recorded in KBr pellet using a Bruker Tensor 27 instrument. Atomic force microscopy of C-dots (Tapping mode, SMART SPM 10000,

AIST-NT) was analyzed by spin coating an aqueous solution of C-dots on freshly cleaved mica surface. The time resolved fluorescence studies were performed on Horiba Yovn (model: Fluorocube-01-NL), a nanosecond time correlated single photon counting (TCSPC) system. Raman spectra were recorded on a Micro Raman system from Jobin Yvon Horiba LABRAM-HR visible with a 632.8 He-Ne laser beam.

## Results and Discussions

In our pursuit towards the development of the nanosensor, we first synthesized luminescent carbon dots by microwave irradiation of a carbon rich precursor  $\beta$ -carotene dispersed in water at elevated temperature. It is worth mentioning that  $\beta$ -carotene is insoluble in water, however microwave irradiation (150 watt) of the orange heterogeneous suspension for 45 minutes at 150°C resulted in a pale yellow solution. The solution exhibited strong fluorescence under UV light ( $\lambda_{\text{ex}}=365$  nm) (Figure S1). The C-dots thus synthesized showed maximum emission at 470 nm when excited at 370 nm and photoluminescence shifted to longer wavelengths with increasing excitation wavelength, a typical characteristic of C-dots (Figure 1a).<sup>22</sup> Atomic force microscopy (AFM) measurements demonstrated the formation of C-dots with particle sizes in the range of 3-6 nm, with their topographic heights mostly between 1 and 2 nm (Figure 1b). Transmission electron microscopy (TEM) also validated the formation of well-dispersed spherical nanoparticles (Figure 1c) and the average diameter as calculated from the particle size histogram was  $3.5 \pm 0.8$  nm (Figure 1d). The high resolution TEM (HRTEM) image of C-dots showed high crystallinity with the appearance of lattice fringes signifying the (102) lattice of graphitic (sp<sup>2</sup>) carbon (Figure S2). The high crystallinity of the C-dots was further supported by the corresponding selected area electron diffraction (SAED) pattern (Figure S3). The synthesized C-dots were highly resistant to photobleaching compared to the commonly used markers such as fluorescein as no rapid photobleaching was observed from the

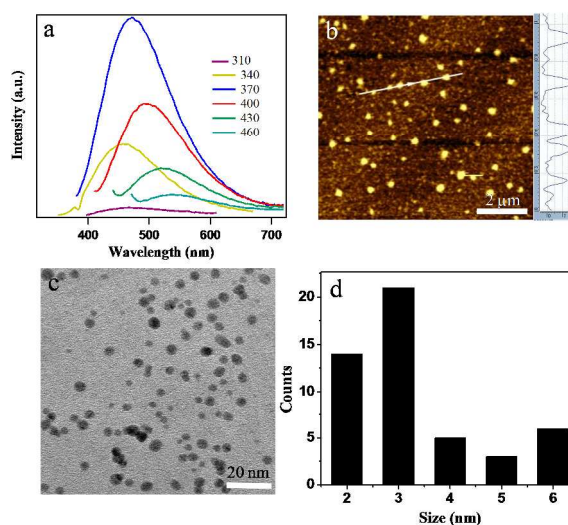


**Fig. 1** (a) Emission spectrum of synthesized C-dots at different excitation wavelengths showing excitation dependent emission, (b) AFM image of the C-dots and corresponding height profile along the line, (c) TEM image and (d) size distribution histogram of the C-dots.

C-dots within 2 hours (Figure S4). Also, the PL time traces of two random spots show gradual intensity decay with no clear photobleaching steps demonstrating that the C-dots are stable for an appreciable time under laser unlike most organic dyes (Figure S5).<sup>48</sup>

The C-dots synthesized by our method exhibited excellent surface reactivity as they efficiently reduced Au<sup>3+</sup> at room temperature. When HAuCl<sub>4</sub> was added to a solution of C-dots in water, the growth of Au NPs was observed colorimetrically within 5 minutes without any heating or photoexcitation. The formation process of Au NPs was allowed for further 30 minutes. The absorption spectrum of C-dots (Figure 2a) showed a narrow peak at 280 nm assigned to the  $\pi \rightarrow \pi^*$  transition of nanocarbon. However in the Au@C-dot composite this characteristic peak disappeared due to the strong electronic interactions between the metal and C-dot.<sup>49</sup> Further the surface plasmon resonance (SPR) band at 528 nm confirmed the formation of Au NPs (Figure 2a). Evidence for the reduction of Au<sup>3+</sup> salts by C-dots was also supported by the dramatic quenching of fluorescence emission of C-dots (Figure 2b). Initially, the carbon dots showed high fluorescence in aqueous solution due to the radiative recombination of the electrons and holes which is generally confined to their surface. During their participation in reducing Au<sup>3+</sup> salts, the nucleation was initiated at the surface sites that host the electrons, thus the process of electron-hole recombination occurring at their surface was hindered leading to effective quenching of the fluorescence emissions.<sup>50</sup> The powder XRD spectra of C-dots exhibited a broad peak centered at  $2\theta = 23^\circ$  corresponding to a d-spacing of 3.8 Å, whereas the Au@C-dot composite showed the characteristic Bragg's reflections corresponding to cubic Au along with the reflection of C-dots (Figure 2c). TEM images showed the formation of a mixture of polyhedral, triangular and rod-like Au nanostructures (Figure S6). A low contrast continuous C-dot layer of thickness ca. 2.6 nm wrapping a high contrast Au core was observed in HRTEM, signifying a core-shell structure (Figure 2d). The SAED pattern of Au@C-dot displayed high crystallinity and the ring patterns corresponding to Au metal with fcc structures were

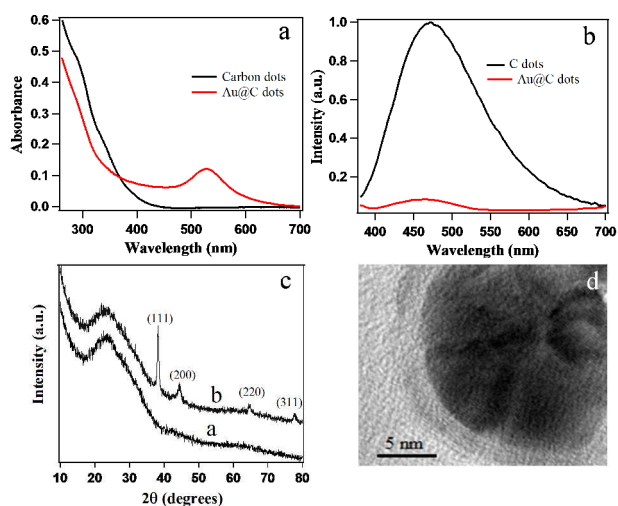


**Fig 2.** (a) UV-visible spectrum of C-dots and Au@C-dots, (b) Emission spectrum of C-dots and Au@C-dots, (c) Powder XRD spectrum of (a) C-dots and (b) Au@C-dots and (d) HRTEM image of Au@C-dots showing a dense Au core coated with a light shell of C-dots.

observed (Figure S7). From the FTIR spectra, it was noticed that the peak at 1710 cm<sup>-1</sup> in case of C-dots became less intense and shifted to 1700 cm<sup>-1</sup> signifying the role of C=O in reduction and binding to Au NPs (Figure S8). Also there was a decrease in the intensity of C-O peak at 1080 cm<sup>-1</sup> suggesting the involvement of C-dots in the reduction process. The Raman spectrum of C-dots did not show any peaks probably due to strong fluorescence background. On the other hand, the Raman spectrum of Au@C-dot composite showed the D-band and G-band of carbon at 1360 cm<sup>-1</sup> and 1530 cm<sup>-1</sup> (Figure S9). The observation of these characteristic bands of carbon in Au@C-dot composite could be attributed to the surface enhancement Raman scattering effect of Au NPs.<sup>27</sup> Further, the observations imply that the strong fluorescence of C-dots was quenched in Au@C-dots due to the electron transfer from the C-dot shells to Au cores, indicating that the C-dots formed a firm coating on Au NP surface.<sup>40</sup> The stability of C-dots and Au@C-dot composites were studied fluorometrically under varying pH, temperature and ionic strength of the medium (details in ESI)<sup>†</sup>.

It is well known that thiols have high binding preference for Au NP surface owing to the formation of a strong Au-S bond.<sup>43-45</sup> Therefore, we presumed that place exchange of C-dots with thiols can take place on the Au NP surface and fluorescence of C-dots could be turned on making Au@C-dot nanocomposites a facile sensor for biothiols. When cysteine (Cys) was added to Au@C-dot composite solution, it turned purple with a considerable red-shift in the plasmon resonance band of Au NPs (Figure 3a). With increasing amount of cysteine, the Au NPs eventually aggregated and precipitated out as observed visually. The aggregation of Au NPs was further confirmed from TEM studies (Figure 3b). Simultaneously, we measured the fluorescence emission of the solution and observed enhancement in fluorescence intensity inherent to C-dots with increasing amount of cysteine (Figure 3c). The enhancement in fluorescence was linearly proportional to

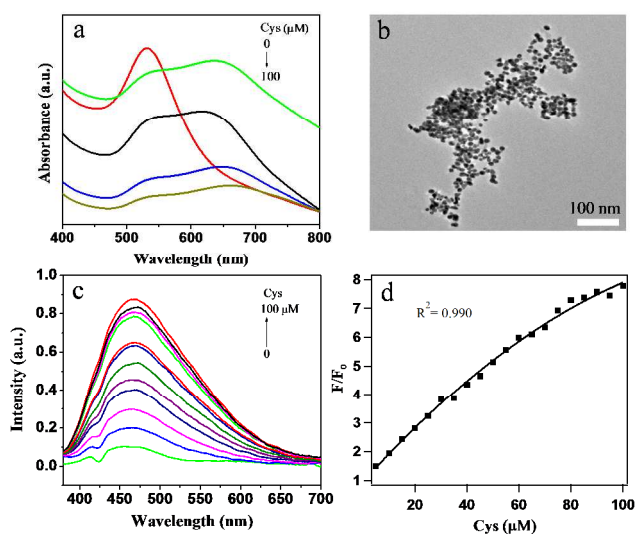


**Fig 3.** (a) UV-visible spectrum of Au@C-dots after addition of various concentrations of cysteine, (b) TEM image of the Au@C-dots showing aggregation after the addition of cysteine, (c) Emission spectrum of the Au@C-dots after addition of different concentrations of cysteine and (d) Relative fluorescence ( $F/F_0$ ) of Au@C-dots as a function of cysteine concentration.

cysteine concentration in the range of 0-30 $\mu$ M (Figure 3d). By using this methodology, we achieved a detection limit of 50 nM within 5 minutes.

In order to establish the mechanism of quenching of fluorescence of C-dots during the formation of Au NPs, Stern-Volmer plot of quenching of C-dot fluorescence at various concentrations of Au<sup>3+</sup> was obtained as shown in Figure 4a. In general, the linearity of Stern-Volmer plot ( $F_0/F$ ) versus the quencher concentration ( $[Q]$ ) indicates that one type of quenching mechanism, static or dynamic, is predominating.<sup>51</sup> The plot was linear at lower concentrations upto  $3 \times 10^{-4}$  M but showed an upward deviation from linearity at higher concentrations which suggested that the quenching process simultaneously followed two mechanisms.<sup>51</sup> One of them is the static quenching in which there is formation of a nonfluorescent complex between fluorophore and quencher in the ground state. The second is dynamic quenching where the fluorophore follows a non-radiative route for the loss of excited state energy which sufficiently alters its lifetime in the excited state. The linear part of fluorescence quenching data (inset, Figure 4a) was analyzed using the Stern-Volmer equation :

$$F_0/F = 1 + K_{SV}[Q]$$

where  $F_0$  and  $F$  denote the fluorescence intensity before and after the quencher addition respectively,  $[Q]$  is the quencher concentration and  $K_{SV}$  is the Stern-Volmer quenching constant which was calculated to be  $1.54 \times 10^4$  M<sup>-1</sup> signifying high quenching efficiency. As reported earlier,<sup>50</sup> the mere presence of Au<sup>3+</sup> does not quench the fluorescence of carbon dots. On the other hand when the C-dots act as electron donors and reduce Au<sup>3+</sup> to Au<sup>0</sup>, their electron rich sites act as nucleating centres for formation of Au NPs. C-dots act simultaneously as a stabilizer for the nanoparticles by forming a layer around them. In this process, the radiative recombinations of electrons and holes at the surface sites of C-dots which are principally responsible for the fluorescence emission are interrupted resulting in diminished fluorescence of C-dots.<sup>50</sup> Thus, Au@C-dot nanocomposites can be considered as nonfluorescent complexes where the Au nanoparticles act as effective fluorescence quenchers.

To gain insights into the dynamic quenching mechanism, TCSPC experiments were performed as shown in Figure 4b. The average lifetime of C-dots was calculated to be 1.910 ns which decreased to 1.003 ns after the formation of Au nanoparticles (Table S1). C-dots show emission in a broad range from 400-600 nm ( $\lambda_{exc} = 370$  nm) and Au nanoparticles have their characteristic absorption band around 475-550 nm which suggests that they can form a donor-acceptor pair of a Förster resonance energy transfer (FRET) system. According to the Förster's energy transfer theory, the energy transfer efficiency for a FRET system depends on the spectral overlap and the distance between the donor and acceptor.<sup>52-53</sup> As can be clearly seen from Figure S13a, the emission spectrum of C-dots shows high overlap with the absorption spectrum of Au nanoparticles leading to efficient FRET which accounts for the reduced lifetime of C-dots. When cysteine was gradually added to the Au@C-dot nanocomposite, we observed that fluorescence owing to C-dots could be regained upto almost 90%. The Au NPs were stabilized by the hydroxyl

and carboxyl functional groups present on the surface of C-dots which are known to bind weakly to the Au NP surface. With the addition of cysteine, a ligand exchange reaction takes place between C-dots and cysteine on Au NP surface, as thiols are known to have higher affinity for metal surfaces.<sup>43-45</sup> This leads to the release of C-dots from the Au surface. Cysteine mediated aggregation of Au nanoparticles leads to rapid broadening and red shift of the SPR band of Au NPs.<sup>54-56</sup> As a result, the spectral overlap of the emission spectrum of C-dots and absorption spectrum of Au NPs becomes less significant (Figure S13b), which also contributes to enhancement in fluorescence due to inefficient FRET. Additionally as more and more Au nanoparticle aggregates are formed with increasing amount of cysteine, the number of effective fluorescence acceptors decreases. Thus, both the ligand exchange and weakened FRET contributed to the recovery of fluorescence of C-dots after the addition of thiol. The binding of thiol to Au NPs was also confirmed by FTIR studies. As can be seen in Figure S14, the peak due to S-H at 2526 cm<sup>-1</sup> in cysteine disappeared when it was bound to Au NPs.

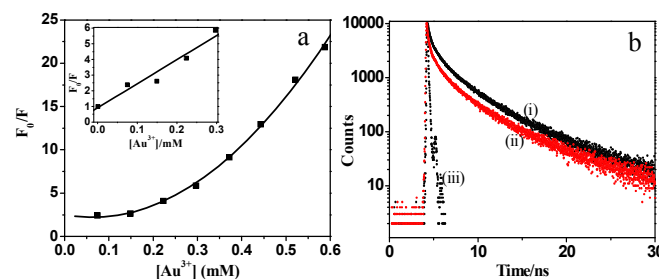


**Fig 4.** (a) Steady state Stern-Volmer plot for the quenching of C-dot fluorescence at various concentrations of Au<sup>3+</sup>; inset: Stern-Volmer plot at lower Au<sup>3+</sup> concentrations and (b) Lifetime decay curves of C-dots (i) in absence and (ii) in presence of  $5.9 \times 10^{-4}$  M Au<sup>3+</sup> ions, (iii) instrument response function.

We performed transmission electron microscopy of Au@C-dot composite after addition of variable amount of cysteine to have a clear insight into the ligand exchange process. Initially the composite particles were well-dispersed (Figure 5a), as C-dot layers acted as stabilizing agents and formed a monolayer around Au NPs. When a small amount of cysteine was added (final concentration 50  $\mu$ M), the C-dots were liberated from the Au surface and the Au NPs started forming a chain like structure (Figure 5b). Clearly the ligand exchange of C-dots with thiols on Au NPs led to release of the C-dots. Subsequent agglomeration of Au NPs was stimulated through electrostatic or hydrogen bonding interactions among cysteine. With higher amount of added cysteine, the Au NPs precipitated out from the solution. Figure 5c shows the TEM image of the Au NP-cysteine aggregates re-dispersed in water depicting the formation of chain like agglomerates of Au nanoparticles. The C-dots released from the Au NP surface remained dispersed in the solution and TEM images (Figure 5d) showed a particle size comparable to those initially synthesized. Also their average lifetime was found to be 1.807 ns which were close to the initial C-dots (Figure S15 and Table S1). From these studies, it was evident that C-dots behave similar to ligands forming self-assembled monolayers.

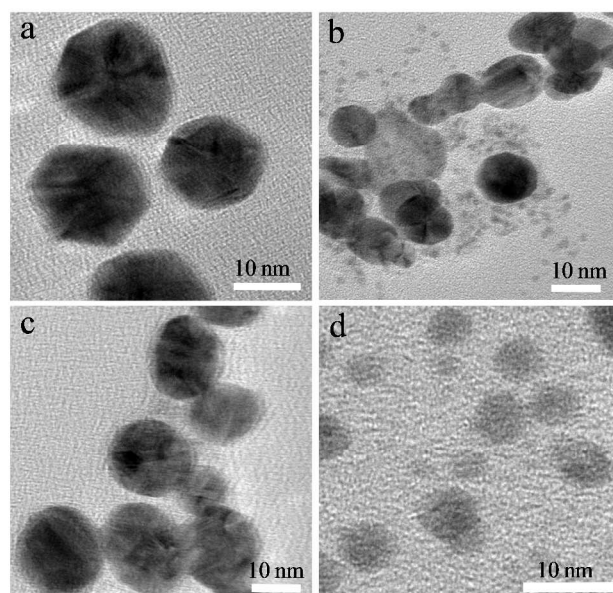


**Fig 5.** (a) TEM image of (a) Au nanoparticles synthesized using C-dots, (b) TEM image of the Au@C-dot composite after addition of 50  $\mu\text{M}$  cysteine, (c) TEM image of the precipitated Au nanoparticles after addition of higher concentration of cysteine and (d) TEM image of the recovered C-dots after addition of higher concentration of cysteine.

It is worth mentioning that other amino acids and commonly occurring biomolecules such as carbohydrates (glucose, fructose etc.) did not lead to any enhancement in fluorescence emission from Au@C-dot composite (Figure 6a). As these amino acids and biomolecules do not contain any free sulfhydryl groups, they can not effectively place exchange the C-dots from Au NP surface. The results suggested that the composite could be used as a fluorometric sensor for thiol containing biomolecules. When we used glutathione, a tripeptide containing free thiol groups, the increment in fluorescence intensity with increasing concentration could be observed (Figure S16). Similar results were obtained with penicillamine, a thiol containing drug molecule (Figure S17). Encouraged by these results, we investigated the specificity of the nanocomposite towards high molecular weight biomolecules containing free sulfhydryl groups, such as proteins and enzymes. Among the four biomacromolecules studied, namely bovine serum albumin (BSA), urease, pepsin and glucose oxidase (GOx), urease showed the maximum fluorescence recovery when incubated with Au@C-dot composite, while GOx showed the minimum fluorescence recovery (Figure 6b). This can be directly correlated to the number of free sulfhydryl groups present in these biomolecules (Table S2). The results (Figure S18) suggested that even high molecular weight macromolecules could effectively replace the C-dots from the Au NP surface, thus establishing Au@C-dot composites as effective sensor for assay of thiol containing macromolecules as well.

To further show the potential utility of the Au@C-dot composites in pharmaceutical samples, we applied this sensing system on two commonly used dietary supplements, becozyme C forte (consists of vitamin B complex and vitamin C) and xtraglo tablets which consists of a variety of vitamins and salts along with an appreciable amount of cysteine. As expected, a solution of xtraglo tablet in water (1.0 mg/mL) when incubated with Au@C-dot nanocomposite led to increase in fluorescence

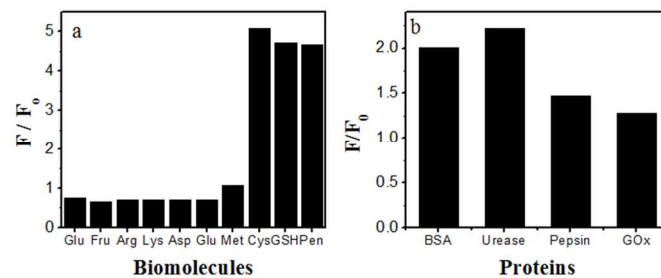


**Fig 6.** Plot of relative intensities of Au@C-dots as a function of (a) different biomolecules and (b) various proteins/enzymes

intensity whereas the pure vitamin supplement did not have any effect (Figure S19).

## 45 Conclusions

In summary, a simple microwave pyrolysis of  $\beta$ -carotene in water afforded highly fluorescent carbon nanodots that could function as an efficient reducing agent for the synthesis of Au NPs at room temperature. The C-dots stabilized the Au NPs by forming a thin continuous layer around the nanoparticle surface. The participation of C-dots as reducing agents led to dramatic quenching of their fluorescence. The quenching is probably due to the nucleation and growth of the nanoparticles at the surface-defect derived energy trapping sites of C-dots leading to disruption of electron-hole recombination processes. The Au@C-dot core shell composites could be used as a dual colorimetric and fluorometric detector for biothiols with high sensitivity and selectivity. The method relies on the fact that the thiol moiety could effectively ligand displace the C-dots from the Au NP surface and the resulting enhancement in fluorescence could be used for quantitative estimation of various biomolecules. Simultaneously the agglomeration of Au NPs induced by the interaction of biomolecules led to red shift of the plasmon resonance band of Au NPs. A detailed investigation into the course of fluorescence turn off and turn on of C-dots revealed a combination of both static and dynamic nature of quenching. It signified that it was not only ligand displacement after cysteine addition in Au@C-dots but also changes in FRET which played an important role. The results are not only important for the development of a nanoparticle based sensor for the reliable diagnosis of biomolecules containing thiols, but also add important support to the current mechanistic framework for fluorescence emissions of C-dots. Further the behavior of C-dots similar to ligands in self-assembled monolayers might open new avenues in potential applications of C-dots.

## Acknowledgements

This research is funded by Science and Engineering Research Board (SERB), Department of Science and Technology, India (SR/S1/PC-32/2010) and Women Scientist Scheme (SR/WOS-A/CS-50/2010). We acknowledge the help from SAIF, NEHU, Shillong for TEM and UGC-DAE Consortium for Scientific Research, Indore for Raman and PXRD facilities. S. M and B. S. acknowledge research fellowships from CSIR and UGC respectively. We thank Dr. Anjan Chakraborty and Mr. Anupam Das for helpful scientific discussions.

## Notes and references

Discipline of Chemistry, School of Basic Sciences, Indian Institute of Technology Indore, IET Campus-DAVV, Khandwa Road, Indore-452017, India. Tel: +91-731-2438706; E-mail: tridib@iiti.ac.in

† Electronic Supplementary Information (ESI) available: [ESI is attached in a separate word file]. See DOI: 10.1039/b000000x/

- U. H. F. Bunz, V. M. Rotello, *Angew. Chem. Int. Ed.* 2010, **49**, 3268-3279.
- A. B. Descalzo, R. Martínez-Mañej, F. Sancenón, K. Hoffmann, K. Rurack, *Angew. Chem. Int. Ed.* 2006, **45**, 5924-5948
- X. Yuan, Y. Tay, X. Dou, Z. Luo, D.T. Leong, J. Xie, *Anal. Chem.* 2013, **85**, 1913-1919.
- B. Hu, Y. Zhao, H. -Z. Zhu, S. -H. Yu, *ACS Nano* 2011, **5**, 3166-3171.
- J. Wang, X. Qu, *Nanoscale* 2013, **5**, 3589-3600.
- M. C. Daniel, D. Astruc, *Chem. Rev.* 2004, **104**, 293-346.
- H. Goesmann, C. Feldmann, *Angew. Chem. Int. Ed.* 2010, **49**, 1362-1395.
- K. Saha, S. S. Agasti, C. Kim, X. Li, V.M. Rotello, *Chem. Rev.* 2012, **112**, 2739-2779.
- W.Y. Chen, C. -C. Huang,; L. -Y. Chen,; H. -T. Chang, *Nanoscale* 2014, DOI: 10.1039/C4NR02817A.
- J. -S. Lee, M. S. Han, C. A. Mirkin, *Angew. Chem. Int. Ed.* 2007, **46**, 4093-4096.
- Y. -L. Hung, T. -M. Hsiung, Y. -Y. Chen, Y. -F. Huang,; C. -C. Huang, *J. Phys. Chem. C* 2010, **114**, 16329-16334.
- D. Liu, Z. Wang, X. Jiang, *Nanoscale* 2011, **3**, 1421-1433.
- J. Zhang, X. Xu, X. Yang, *Analyst* 2012, **137**, 1556-1558.
- X. Xie, W. Lu, X. Liu, *Acc. Chem. Res.* 2012, **45**, 1511-1520.
- P. Liu, X. Yang, S. Sun, Q. Wang, K. Wang, J. Huang, J. Liu, L. He, *Anal. Chem.* 2013, **85**, 7689-7695.
- H. Zheng, S. Qiu, K. Xu, L. Luo, Y. Song, Z. Lin, L. Guo, B. Qiu, G. Chen, *Analyst* 2013, **138**, 6517-6522.
- F. Xia, X. Zuo, R. Yang, Y. Xiao, D. Kang, A. Vallée-Béllisle, X. Gong, J. D. Yuen, B. B. Y. Hsu, A. J. Heeger, K. W. Plaxco, *Proc. Nat. Acad. Sci. USA* 2010, **107**, 10837-10841.
- G. H. Woehrle, L. O. Brown, J. E. Hutchison, *J. Am. Chem. Soc.* 2005, **127**, 2172-2183.
- Y. Zhou, S. Wang, K. Zhang, X. Jiang, *Angew. Chem. Int. Ed.* 2008, **47**, 7454-7456.
- Y. -R. Kim, R. K. Mahajan, J. S. Kim, H. Kim, *ACS Appl. Mater. Interfaces* 2010, **2**, 292-295.
- L. Chen, W. Lu, X. Wang, L. A. Chen, *Sensors and Actuators B* 2013, **182**, 482-488.
- H. Li, Z. Kang, Y. Liu, S. -T. Lee, *J. Mater. Chem.* 2012, **22**, 24230-24253.
- H. Li, X. Hi, Z. Kang, H. Huang, Y. Liu, J. Liu, S. Lian, C. H. A. Tsang, X. Yang, , S. -T. Lee, *Angew. Chem. Int. Ed.* 2010, **49**, 4430-4434.
- Z. Ma, Y. -L. Zhang, L. Wang, H. Ming, H. Li, X. Zhang, F. Wang, Y. Liu, Z. Kang, S. -T. Lee, *ACS Appl. Mater. Interfaces* 2013, **5**, 5080-5084.
- H. Ming, Z. Ma, Y. Liu, K. Pan, H. Yu, F. Wang, Z. Kang, *Dalton Trans.* 2012, **41**, 9526-9531.
- R. Liu, J. Liu, W. Kong, H. Huang, X. Han, X. Zhang, Y. Liu, Z. Kang, *Dalton Trans.* 2014, **43**, 10920-10929.
- R. Liu, H. Huang, H. Li, Y. Liu, J. Zhong, Y. Li, S. Zhang, Z. Kang, *ACS Catal.* 2014, **4**, 328-336.
- S. N. Baker, G. A. Baker, *Angew. Chem. Int. Ed.* 2010, **49**, 6726-6744.
- P. G. Luo, S. Sahu, S. -T. Yang, S. K. Sonkar, J. Wang, H. Wang, G. E. LeCroy, L. Cao, Y. -P. Sun, *J. Mater. Chem. B* 2013, **1**, 2116-2127.
- M. P. Sk, A. Jaiswal, A. Paul, S. S. Ghosh, A. Chattopadhyay, *Sci. Rep.* 2012, **2**, 383, DOI:10.1038/srep00383.
- H. Zhang, H. Huang, H. Ming, H. Li, L. Zhang, Y. Liu, Z. Kang, *J. Mater. Chem.* 2012, **22**, 10501-10506.
- P. Anilkumar, L. Cao, J. -J. Yu, K. N. Tackett II, P. Wang, M. J. Meziani, Y. -P. Sun, *Small* 2013, **9**, 545-551.
- S. K. Bhunia, A. Saha, A. R. Maity, S.C. Ray, N. R. Jana, *Sci. Rep.* 2013, **3**, 1473, DOI:10.1038/srep01473.
- S. Karthik, B. Saha, S. K. Ghosh, N. D. P. Singh, *Chem. Commun.* 2013, **49**, 10471-10473.
- C. Ding, A. Zhu, Y. Tian, *Acc. Chem. Res.* 2014, **47**, 20-30.
- C. Hu, C. Yu, M. Li, X. Wang, J. Yang, Z. Zhao, A. Eychmüller, Y. -P. Sun,; J. Qiu, *Small* 2014, DOI: 10.1002/smll.201401328.
- L. Zhou, Y. Lin, Z. Huang, J. Ren, X. Qu, *Chem. Commun.* 2012, **48**, 1147-1149.
- C. Shen, Y. Sun, J. Wang, Y. Lu, *Nanoscale* 2014, **6**, 9139-9147.
- H. Li, J. Liu, M. Yang, W. Kong, H. Huang, Y. Liu, *RSC Adv.* 2014, **4**, 46437-46443.
- P. Luo, C. Li, G. Shi, *Phys. Chem. Chem. Phys.* 2012, **14**, 7360-7366.
- X. Qin, W. Lu, A. M. Asiri, A. O. Al-Youbi, X. Sun, X. Green, *Catal. Sci. Technol.* 2013, **3**, 1027-1035.
- D. Dey, T. Bhattacharya, B. Majumdar, S. Mandani, B. Sharma, T. K. Sarma, *Dalton Trans.* 2013, **42**, 13821-13825.
- H. S. Jung, X. Chen, J. S. Kim, J. Yoon, *Chem. Soc. Rev.* 2013, **42**, 6019-6031.
- S. -J. Chen, H. -T. Chang, *Anal. Chem.* 2004, **76**, 3727-3734.
- J. Wang, Y. F. Li, C. Z. Huang, T. Wu, *Anal. Chim. Acta.* 2008, **626**, 37-43.
- B. Han, E. Wang, *Biosens. Bioelectron.* 2011, **26**, 2585-2589.
- O. Demirkol, C. Adams, N. J. Erkal, *Agric. Food Chem.* 2004, **52**, 8151-8154.
- E.P. Ippen, C.V. Shank, A. Dienes, *IEEE J. Quantum Electron.* 1971, **QE-7**, 178-179.
- S.S. Mandal, U. Varshney, S. Bhattacharya, *Bioconjugate Chem.* 1997, **8**, 798-812.
- J. Xu, S. Sahu, L. Cao, C. E. Bunker, G. Peng, Y. Liu, K. A. S. Fernando, P. Wang, E. A. Gulians, M. J. Meziani, H. Qian, Y. -P. Sun, *Langmuir* 2012, **28**, 16141-16147.
- J. R. Lakowicz, *Principles of Fluorescence Spectroscopy*, Springer, New York, USA 2006.
- M. A. H. Muhammed, A. K. Shaw, S. K. Pal, T. Pradeep, *J. Phys. Chem. C* 2008, **112**, 14324-14330.
- G. Chen, F. Song, X. Xiong, X. Peng, *Ind. Eng. Chem. Res.* 2013, **52**, 11228-11245.
- F. X. Zhang, L. Han, L. B. Israel, J. G. Daras, M. M. Maye, N. K. Ly, C. -J. Zhong, *Analyst* 2002, **127**, 462-465.
- S. Basu, S. Panigrahi, S. Prharaj, S. K. Ghosh, S. Pande, S. Jana, T. Pal, *New J. Chem.* 2006, **30**, 1333-1339.
- A. Mocanu, I. Cernicab, Gh. Tomoaia, L. -D. Bobosa, O. Horovitz, M. Tomoaia-Cotisel, *Colloids Surf. A: Physicochem. Eng. Aspects* 2009, **338**, 93-101.